

An Assessment of Algorithms to Estimate Respiratory Rate from the Remote Photoplethysmogram

Duncan Luguern¹, Simon Perche¹, Yannick Benezeth¹, Virginie Moser²

L. Andrea Dunbar², Fabian Braun², Alia Lemkadem², Keisuke Nakamura³, Randy Gomez³, Julien Dubois¹

¹ Univ. Bourgogne Franche-Comté, Dijon, France

² CSEM, Neuchâtel, Switzerland

³ Honda Research Institute Japan Co., Honcho, Wako-shi, Saitama, Japan

Abstract

The respiratory rate is important information in the healthcare environment. Consequently, research is done to develop a device that could measure the respiratory rate continuously with non-contact devices. Various methods were tried, such as radio-based, thermal imaging or remote photoplethysmography (rPPG). The rPPG method uses a video recording of the skin in ambient light conditions. It measures the small variations of light reflection induced by the amount of blood in vessels. This method allows the extraction of physiological parameters such as the heart rate or respiratory rate without any contact with the skin. The main issue with the rPPG technique is the lower signal quality compared with contact-based methods. In this paper, we assess the performance of the respiratory rate estimation algorithms with rPPG signals. The tested algorithms were designed for contact-PPG signals input. The use of the algorithms designed for contact PPG on remote PPG signals can lead to respiratory rate estimations with a mean absolute error below 3 breaths-per-minute. We benchmark our results using this standard and some other metrics to interpret the quality of the assessment.

1. Introduction

The estimation of the respiratory rate is often neglected by the medical staff. It is a time-consuming measurement and inconvenient to be performed [1]. Indeed, the gold standard for respiratory rate assessment is a 1-minute manual measure [2]. However, this measure provides early information about medical complications. For example, cardiac arrest [3], ischemic stroke [4], and state of shock [5] can be better detected considering respiratory rate information. So its assessment should be as frequent and robust as possible. Many contact-based measurement methods were developed to measure the respiratory rate continuously. The

impedance pneumography, respiratory belts or capnography have been the first systems to be developed to perform such measurements. They obtain accurate results, unfortunately, continuous use of such systems is uncomfortable. Moreover, they are too bulky to be used daily.

To address these issues, some technologies were used to provide wearable devices. Electrocardiography (ECG) [6, 7] and photoplethysmography (PPG) [8, 9] based respiratory rate extraction are promising for continuous monitoring. The ECG devices consist of electrodes fixed to the skin. These electrodes measure the electrical field induced by the heart and respiratory activity in the chest. The PPG devices use the light absorption of the skin to estimate a blood volume signal. Light passes through the skin and is modulated by the blood contained in the vessels. This allows measuring the variation of the blood in the vessels. From this signal, it is also possible to get respiratory information. Contrary to previous methods, they can be implemented in wearable devices such as smartwatches to monitor physiological parameters outside the healthcare environment [10, 7]. The main issue with these techniques is the need for contact with skin. This need is troublesome as it may cause some discomfort and hygiene issues on fragile skins.

Several non-contact based methods were developed to solve these issues. For example, radio-based methods [11, 12], movement-based methods [13, 14] or thermal imaging-based methods [15, 16] are currently investigated. These methods are less robust than contact-based methods because of the noise introduced by movements or the environment. Some of these also need high-cost devices that curb their usage.

Another non-contact method, called remote photoplethysmography (rPPG) uses a camera and the light reflection from the skin to extract blood volume pulse signals. This technique can be employed with a low-cost webcam and ambient light for the heart rate estimation [17, 18].

The principles of this method are similar to the contact PPG method. It measures the light that is reflected from the skin and from this deduces the blood circulation as the light is more or less absorbed depending on the amount of blood in vessels. The light fluctuation, and therefore the resulting measurement contains cardiac information as well as respiratory information [19, 20]. The general processing steps needed to get a respiratory rate from video recordings are shown in figure 1.

To get an rPPG signal, the video is first segmented in skin and non-skin pixels. This step often consists of face detection and tracking, plus a skin pixel detection to refine the signal's quality. A spatial averaging is done on the skin pixels to get the color traces. These color traces are combined to enhance the quality of the physiological signal and to reduce the noise. The combination methods can use either the statistical properties of the traces or the light-tissue interaction properties to get a signal. The statistical properties-based methods are PCA [18], ICA [21], PVM [22] and EVM [23] methods. PCA creates a rotation matrix that separates the principal components embedded in the color traces. The principal components are as uncorrelated as possible. ICA tries to maximize the non-gaussianity and thus the independence of the output signal. PVM and EVM are based on the GEVD algorithm [24]. They construct a rotation matrix that maximizes a ratio of properties. The property used in PVM is the periodicity of the signal, while the one used in EVM is its SNR. The other class of methods, such as CHROM or PBV, employs the physiological properties of the light/skin tissue interaction to improve the quality of the signal. CHROM [25] chooses a combination that is orthogonal with the specular reflection component. PBV [26] is based on a similar principle as CHROM but uses a so-called blood volume pulse component on which the color traces are projected.

The obtained 1D signal is the rPPG pulse trace. It is similar to the contact PPG signal often with a lower quality. This signal can be then analyzed to extract physiological information. The respiratory information can be extracted from rPPG signals using similar techniques as with PPG signals. Breathing modulates the (r)PPG signals in three ways. First, an additive modulation called *baseline wander* occurs, due to variation in the intrathoracic pressure. Secondly, the amplitude of cardiac pulses varies with respiration because of the changes in the cardiac refill. This is called *amplitude modulation*. Finally, *frequency modulation* is caused by the modification of intrathoracic pressure. This change causes a physiological response called Respiratory Sinus Arrhythmia (RSA) that can be revealed in (r)PPG signal as a small variation in the instantaneous heart rate.

A lot of algorithms were developed to assess the respiratory rate from a PPG signal. Charlton *et al.* [27] reviewed most of these algorithms in a single framework to predict

which algorithm is best suited for the respiratory rate assessment with contact PPG signals. In this paper, we considered the work presented by Charlton *et al.* to benchmark the respiratory rate assessment from rPPG signals. To do this, we extracted the RGB traces from videos and combined them using four state-of-the-art combination algorithms. These algorithms were parametrized to output either a *baseline wander* respiratory signal or a cardiac signal carrying *amplitude modulation* and *frequency modulation*. These signals were then used as input of the framework to extract the respiratory rate of the subjects. The algorithms used in this analysis are presented in 2. The details of our implementation and parameters are detailed in 3. Then, section 4 shows the results obtained and their analysis.

2. Methods

In this section we present the algorithms used for the respiratory rate estimation. First, the color traces combination algorithms are presented and their variation for cardiac/respiratory signal enhancement is detailed. Then, Charlton's respiratory rate extraction algorithms are presented. Finally, the implementation details of the complete pipeline and the metrics used for the method comparison are shown.

2.1. Combination algorithms

The combination algorithms used to get the pulse or respiratory signal are CHROM [25], PBV [26], PVM [22] and EVM [23]. The CHROM and PBV algorithms use a pre-computed vector to guide the combination. The vector is either the specular reflection component in the CHROM case or a blood volume pulse vector direction for PBV. The goal of CHROM is to remove the information carried by this vector by projecting the color traces on the components orthogonal to the noise-carrying vector. The PVM and EVM methods use a combination using only the frequency characteristics of the color traces. The drawback of these methods is that a periodic noise can confuse them. The PVM method estimates a rotation matrix with the first output component showing the highest periodicity. On a similar idea, the EVM algorithm maximizes the SNR of the first output component. The SNR is considered as the energy of a filtered signal over the non-filtered signal. The EVM procedure is then refined to update the tracked frequency and the rotation matrix on each new sample, using an adaptive filter.

These algorithms can be used to get a respiratory or cardiac signal, depending on the frequency band they consider as the signal. To extract the respiratory signal from the color traces, the CHROM algorithm uses the combination vector obtained with a frequency band including the pulse rate. This vector is reemployed on a low-frequency band traces to get a respiratory signal. The same approach is used with PBV. A complete description of the processing pipeline can

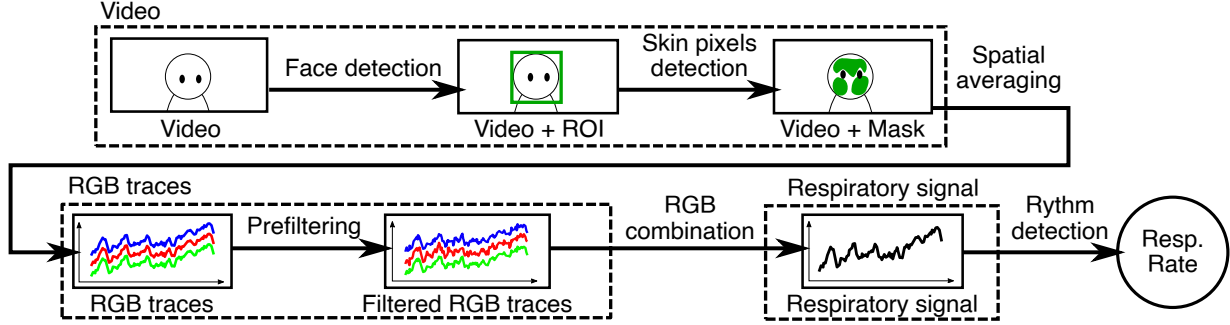


Figure 1. The general rPPG processing pipeline to estimate respiratory rate from video recordings.

be found in [28]. The EVM and PVM algorithms are used directly on the color traces filtered with a band-pass filter keeping the respiratory signal. Depending on the chosen parameters, these algorithms can either output a respiratory signal or a cardiac signal. In this paper we note “respiratory rPPG” the respiratory signal obtained from the combination step output, and “cardiac rPPG” the cardiac signal obtained from the combination algorithms and as the input of Charlton’s respiratory signal extraction algorithms.

2.2. Respiratory rate extraction algorithms

The respiratory rate extraction code is publicly available in [27]. To assess the performance of our algorithms, we implemented the processing pipeline summarized in figure 3. The combination algorithms output either a cardiac rPPG signal or a respiratory rPPG signal. The cardiac signals are processed with respiratory signal extraction of Charlton’s framework to obtain respiratory signals. These signals and the respiratory rPPG signals are then analyzed with the respiratory rate estimation and the modulation fusion algorithms presented in Charlton’s work. In next paragraphs we refer to Charlton’s algorithms using the naming convention presented in [27]. In this convention, the X algorithm family refers to the respiratory signal extraction step. The A and B subfamilies group the filter-based and the feature-based extraction algorithms respectively. The E letter names the respiratory rate estimations class algorithms. The F subletter indicates a frequency-based technique and the T subletter indicates a time-domain-based technique. Finally, the respiratory rate fusion and smoothing algorithms are named with the F letter. The modulation fusion class algorithms have the M subletter and the temporal smoothing class algorithms have the T subletter.

2.2.1. Cardiac signal to respiratory signal extraction.

The cardiac rPPG signals are first used for respiratory signal extraction. This can be done using filter-based or feature-based algorithms. Charlton presented 12 extraction algorithms with a PPG input. The filter-based extraction algorithms are bandpass-filter based (X_{A1} [29]), Continuous

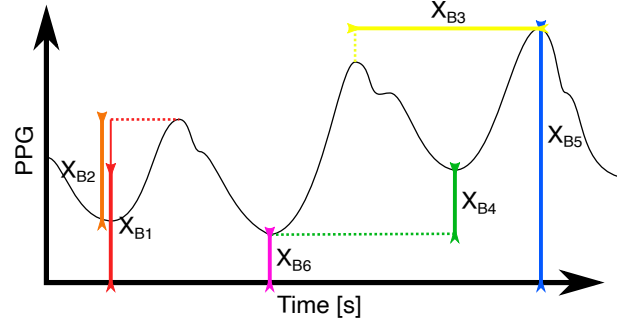


Figure 2. Peak-troughs detection-based algorithms example.

Wavelet Transform based (X_{A2} and X_{A3} [30]) or centered-correntropy function based (X_{A4} [31]). The feature-based algorithms can be split in peak/troughs detection-based algorithms, kernel PCA algorithm, and pulse width measurement algorithm. In the feature-based algorithms, an initial step consists of peak and trough detection with the Incremental Merge Segmentation algorithm [32]. The features obtained from the peak/troughs detection algorithm are summarized in figure 2 [32, 33, 34]. The figure shows that X_{B1} is the mean of a peak/trough pair (*baseline wander*). The X_{B2} algorithm measures the amplitude of the pulse. X_{B3} is a *frequency modulation* based algorithm that measures the time delay between two successive peaks. X_{B4} is the amplitude difference between consecutive troughs. The X_{B5} and X_{B6} respectively measures the peak and the trough amplitude. The X_{B7} and X_{B8} algorithms are dedicated to ECG signals and thus are not considered in this study. The X_{B9} [35] algorithm uses a kernel PCA method. It constructs a matrix with signal slices. Each slice is centered on a detected trough. The best Eigenvector is used to recombine these slices and generate a respiratory signal. The X_{B10} [36] algorithm measures the PPG pulse width using a wave boundary detection algorithm.

Once the feature metrics are obtained, a resampling step creates a uniform sampled signal. The resampling algorithms are *cub*, *cubB*, *lin* and *linB*. They are a cubic and linear interpolation. The B suffix indicates that the result-

ing signal was bandpass filtered at physiological frequencies. The resampling step is used on cardiac rPPG processing with X_{B*} algorithms. Indeed, these algorithms output irregularly sampled respiratory signals that need to be resampled for the next steps.

2.2.2. Respiratory rate estimation. To make this section easier to read, we will refer to “cardiac rPPG” as the combination made to enhance the cardiac signal quality that is processed by Charlton’s algorithms to get a respiratory signal, and “respiratory rPPG” as the combination made to enhance the respiratory signal quality. In previous step, the respiratory signal was extracted from the cardiac rPPG signal. The respiratory rPPG signals are included in the processing framework at this step. This part consists of estimating the respiratory rate from the signal. Charlton’s framework contains 12 algorithms dedicated to respiratory rate extraction. These are frequency-domain based or time-domain based techniques. They convert windows using frequency analysis techniques and detect respiratory frequency in the spectrum. E_{F1} [32] uses a Fast Fourier Transform. The respiratory rate is the frequency with the highest energy in the frequency band. A similar procedure is done in E_{F6} [37], using FFT on the autocorrelation of the signal. The E_{F2} [33, 38], E_{F3} [39], E_{F4} [40], E_{F5} [41] algorithms analyze the window using a Burg’s autoregressive (AR) model. E_{F2} employs a peak detection procedure on the order-8 AR power spectral density. Similarly, E_{F4} computes AR power spectral density with varying orders. E_{F3} and E_{F5} compute the poles of the order-8 model and search for the valid poles in the physiological frequencies. This can be either the highest pole or the lowest frequency pole, with the magnitude being more than 95% of the highest pole. Finally, the E_{F7} [36] algorithm uses a Welch periodogram.

The time-domain techniques generally use peak and/or trough detection to estimate the respiratory rate. The E_{T1} [42] algorithm defines the duration used to compute the respiratory rate as the delay between the first and the last detected peak. In E_{T3} [43] a filtering part is added. The E_{T5} [37] algorithm uses the amplitude difference of pairs of extremes to filter peaks and troughs. E_{T4} [37] filters troughs that are above 0 and peaks that are below a threshold. Finally, the E_{T2} [44] algorithm computes zero-crossing events and get the respiratory rate as the zero-crossing frequency.

2.2.3. Modulation fusion. An optional last step consists of a fusion of the respiratory rhythms detected with the three physiological modulations. In Charlton *et al.*, this step improved significantly the quality of the assessment. The presented algorithms are smart fusion F_{M1} [32], spectral peak-conditioned averaging F_{M2} [36], pole magnitude criterion F_{M3} [33] and pole ranking criterion F_{M4} [45]. In this study the temporal smoothing algorithm was not evaluated.

3. Experimental protocol

3.1. Implementation details

The code was executed using Matlab [46]. To allow a more robust comparison between the algorithms, we used the same steps to extract color traces for each combination algorithms. Using a video, the code detects face using Viola-Jones algorithm [47] and tracks its movements using Kanade-Lucas-Tomasi algorithm [48]. A skin pixel detection step is implemented using a histogram matching algorithm [49]. The previously defined region-of-interest is spatially averaged to get the color traces. These color traces are normalized using the procedure described in CHROM [25]. The choice of window length was 8 seconds for CHROM, PBV and PVM and 2-seconds for EVM. The 8-seconds window was used with respect to the CHROM article [28], while the 2-seconds window showed better results with the EVM algorithm [23]. The 8-seconds window length confuses EVM when the respiratory rate is at about 15 rpm (respirations-per-minute). Using an empirically fixed 2-seconds window improved the results on this frequency band. The CHROM and PBV algorithms are implemented according to [28] without the sub-regions and weighting steps that are not relevant in this study. The scaling and windowing steps are kept. PVM is computed on 30-seconds windows with a 1-second step between windows, in line with the original paper [22]. A similar scaling/windowing procedure as in CHROM is made with PVM.

3.2. Charlton pipeline adaptation

Some modifications were made to use the rPPG signals inside Charlton’s framework. The respiratory signal extraction step is executed on cardiac rPPG signals only. An adaptation of the parameters is needed to deal with the lower sampling frequency of the rPPG signals (20 Hz in the dataset). Thus, the downsample steps were disabled because the sampling frequency was low enough for most processing. Charlton’s framework assesses the algorithms performance using the intermediate signals generated during the process. However, these intermediates signals are missing in the case of the respiratory rPPG signals. So the signal quality index and the statistics obtained at the end of the framework were disabled.

3.3. Database

The database used for validation of the framework is the Newborn Care Adult database made by the CSEM of Neuchâtel (Switzerland) [50]. The database consists of three scenarios with 12 subjects per scenario. The heart rate and respiratory rate ground truth values are recorded using ECG, PPG and respiratory belt. The management of the ground truth values is done using a TSD201 Biopac Systems, Inc., USA® device. All videos show a subject

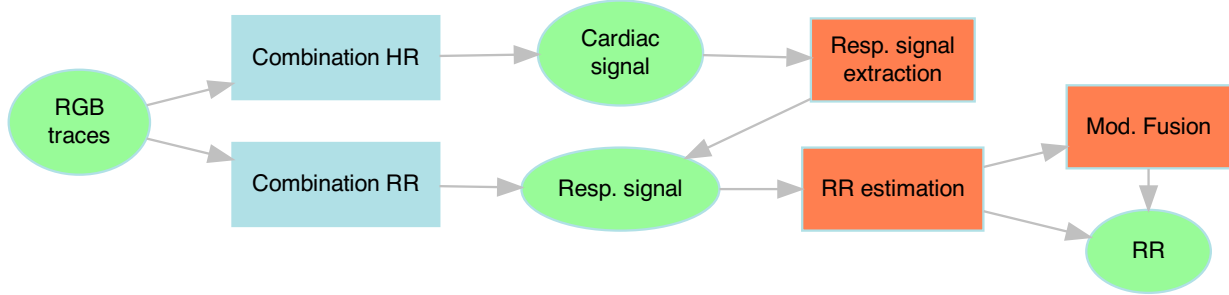


Figure 3. The processing pipeline from rPPG signals to respiratory rate.

face and upper body. The subjects are laying on a hospital bed with sensors attached to their body. The HandGrip scenario shows a subject doing a handgrip exercise to accelerate its heart rate. The Respiration scenario challenges the respiratory rate estimation with an initial apnea and increasing respiratory rates from 5 to 15 rpm. In the Movement scenario, the subject is asked to move the head laterally during the record. The videos were recorded using an RGB camera with artificial light illumination. They are at 20 fps and 1280×1024 pixels size with a resolution of 1.3 Mp, without compression. The apnea segment in the Respiration scenario was removed to assess the performance of the algorithms in detecting respiratory rates (not detecting apneas). The respiratory rate estimation for the HandGrip ground truth signals failed with subjects 6 and 7. These subjects were ignored in the HandGrip database to have a better comparison of the algorithms.

4. Results and discussion

To assess the performance of the processing pipelines (RGB combination, respiratory signal extraction, respiratory rate estimation and respiratory rate smoothing algorithms), we define five metrics: r , $Prec\ 1$, $Prec\ 2$, MAE and $RMSE$. The r metric is the Pearson coefficient. The $Prec\ 1$ and $Prec\ 2$ metrics are the number of rhythms with an absolute error smaller than a given threshold, over the total number of rhythms. The thresholds are respectively 1 and 2. The Mean Absolute Error (MAE) metric shows the average of the absolute difference between the ground truth and the estimated rhythms. The Root Mean Square Error ($RMSE$) computes the average of the squared difference between ground truth and estimated rhythms and gives the square root of it.

To compare the results, we extracted for each scenario the 10 best processing pipelines, based on their MAE. These results are presented in table 1, 2 and 3. As presented in 2, the *Resample* step concerns only signals extracted with the X_{B*} algorithms family. Moreover, the *Extract* step is only used to extract a respiratory signal from cardiac rPPG signal. The *HR/RR* column indicates if the signal obtained with the combination algorithm is either a cardiac rPPG signal or

a respiratory rPPG signal. The best results are presented in bold.

The Respiration scenario can get significant results using EVM or PVM with a modulation fusion step. The resampling algorithm does not significantly change the results. The best respiratory rate estimation algorithm class are frequency-based for EVM with an autocorrelation model-based algorithm (E_{F3}) and temporal-based for PVM (E_{T2} and E_{T3}).

In the Movement scenario, the combination algorithm that gave the best results is CHROM and PVM. However, PVM seems to have a low r value, so we consider ignoring it in the interpretation of the results. The results of CHROM with this scenario is coherent with the literature, while this algorithm is designed to suppress the movement-correlated noise produced by the specular component of the light. The EVM and PVM algorithms detect a frequency or a period of interest and enhance it. Thus movement polluted signals may confuse these algorithms and lead to bad results. The respiratory signal extraction algorithms are mostly feature-based. The best feature-based algorithm was X_{B3} which corresponds to the *frequency modulation*. The modulation fusion algorithm can get good results too, however it seems that the use of frequency modulation is sufficient by itself. The best respiratory rate estimation algorithms were time-domain, mostly E_{T1} and E_{T2} . Finally, the MAE is higher than in the Respiration database. This is coherent considering that the Movement database has a more challenging setup.

In the HandGrip scenario, the results seems to be intermediate between the Respiration and Movement database results. This is in line with the setups, while Respiration database is supposed to be the easiest database and Movement the hardest to process. The best combination algorithms are CHROM, PBV and PVM. It seems that the combination step is not very important in this setup. However, best pipelines produce the respiratory signal directly. The other pipelines use modulation fusion algorithms F_{M1} and F_{M2} to improve the estimation quality. The best respiratory rate estimation algorithms were E_{F2} and E_{F3} . They are all frequency-based. They are all based on an AR model

Combine	Resample	Extract	Estimate	Mod. Fusion	HR/RR	r	Prec 1	Prec 2	MAE	RMSE
EVM	lin		E_{F3}	F_{M2}	Both	0.65	0.27	0.52	2.27	3.48
EVM	cub		E_{F3}	F_{M2}	Both	0.65	0.27	0.52	2.27	3.47
PVM	linB		E_{T2}	F_{M1}	Both	0.78	0.17	0.33	2.28	2.89
PVM	lin		E_{T3}	F_{M1}	Both	0.74	0.14	0.29	2.34	3.01
PVM	cub		E_{T3}	F_{M1}	Both	0.74	0.14	0.28	2.34	3.00
PVM	lin		E_{T2}	F_{M1}	Both	0.74	0.16	0.29	2.37	3.06
PVM	cub		E_{T2}	F_{M1}	Both	0.74	0.15	0.28	2.37	3.06
PVM	linB		E_{T3}	F_{M1}	Both	0.76	0.15	0.30	2.37	2.95
PVM	cubB		E_{T2}	F_{M1}	Both	0.77	0.15	0.28	2.39	2.96
PVM	cubB		E_{T3}	F_{M1}	Both	0.74	0.14	0.27	2.41	2.99

Table 1. The 10 best algorithms for Respiration database, ordered by their MAE.

Combine	Resample	Extract	Estimate	Mod. Fusion	HR/RR	r	Prec 1	Prec 2	MAE	RMSE
PVM	lin		E_{T1}	F_{M1}	Both	0.03	0.04	0.08	4.14	5.41
PVM	cub		E_{T1}	F_{M1}	Both	-0.01	0.04	0.08	4.23	5.54
PVM	linB		E_{T1}	F_{M1}	Both	0.25	0.03	0.07	4.58	5.82
CHROM	lin	X_{B3}	E_{T2}		HR	0.37	0.10	0.26	4.64	5.64
CHROM	lin		E_{T2}	F_{M1}	Both	0.31	0.10	0.16	4.64	5.48
CHROM	linB		E_{T2}	F_{M1}	Both	0.29	0.07	0.13	4.64	5.40
CHROM	cub	X_{B3}	E_{T2}		HR	0.37	0.10	0.25	4.68	5.64
CHROM	cub		E_{T2}	F_{M1}	Both	0.28	0.09	0.15	4.70	5.47
CHROM	cubB		E_{T3}	F_{M1}	Both	0.23	0.08	0.15	4.70	5.53
CHROM	cubB		E_{T2}	F_{M1}	Both	0.21	0.07	0.16	4.73	5.65

Table 2. The 10 best algorithms for Movement database, ordered by their MAE.

method.

Considering the results from a global point of view, we see that depending on the scenario it is possible to improve the quality of the assessment with a careful choice of the algorithm. This choice is lead by the quality of the respiratory signal and of the cardiac signal. Videos with high quality of respiratory signals in the color traces should use the EVM or PVM methods to get a respiratory signal. On the other side, videos with high quality of cardiac signal or movement-induced noise should use the CHROM or PBV method to extract the respiratory signal. The best respiratory signal extraction algorithm is feature-based and represents the *frequency modulation*. The respiratory rate estimation techniques use either time-domain methods with the E_{T2} and E_{T3} and frequency-domain methods with E_{F2} and E_{F3} which are autoregressive model-based. In most of the pipelines, the use of a modulation fusion improved significantly the results. This is in line with Charlton’s conclusions. On the other hand, Charlton concluded that the best respiratory rate estimation techniques were time domain. In our results we show that frequency-domain techniques can also obtain significant results. Further work should be made to

confirm these results on other setups.

The detected rhythms are presented using Bland-Altman (figure 4) and correlation plots (figure 5). Some outliers were in the EVM algorithm with an estimated rhythm higher than 30 rpm and have been removed on the correlation plots to improve the readability. Also, a red area is drawn to show a local mean absolute error computed on the neighborhood of a mean frequency for the Bland-Altman plot (ground truth frequency for the correlation plot). The window used to compute the mean error is of ± 1 rpm. Another annotation is the histogram of the estimated respiratory rhythms. This annotation is shown on the right margin of the Bland-Altman plot.

We use Respiration scenario rhythms to get a look at all physiological frequencies. The selected algorithms are *CHROM lin X_{B3} E_{T2} HR*, *EVM lin E_{F3} F_{M2} Fus*, *PVM lin E_{T3} F_{M1} Fus* and *PBV E_{F2} RR*. In this nomenclature the first word indicates the combination algorithm, the last word indicates the kind of signal obtained with the combination algorithm. The X^* and E^* methods are Charlton’s respiratory signal and respiratory rate extraction algorithms, respectively. If needed, the resampling function

Combine	Resample	Extract	Estimate	Mod.	Fusion	HR/RR	r	Prec 1	Prec 2	MAE	RMSE
CHROM			E_{F3}			RR	0.33	0.21	0.41	3.03	3.78
PVM			E_{F2}			RR	0.35	0.20	0.39	3.04	3.69
PBV	lin		E_{F2}		F_{M2}	Both	0.34	0.17	0.33	3.05	3.72
PVM			E_{F3}			RR	0.30	0.21	0.40	3.05	3.73
PBV	cub		E_{F3}		F_{M2}	Both	0.27	0.20	0.38	3.05	3.85
PBV	lin		E_{F3}		F_{M2}	Both	0.26	0.20	0.38	3.05	3.86
PBV	cub		E_{F2}		F_{M2}	Both	0.35	0.18	0.33	3.06	3.73
PBV	cubB		E_{F2}		F_{M1}	Both	0.06	0.14	0.31	3.06	3.74
CHROM	lin		E_{F3}		F_{M2}	Both	0.28	0.19	0.39	3.08	3.77
PBV	linB		E_{F2}		F_{M1}	Both	0.04	0.15	0.33	3.09	3.77

Table 3. The 10 best algorithms for HandGrip database, ordered by their MAE.

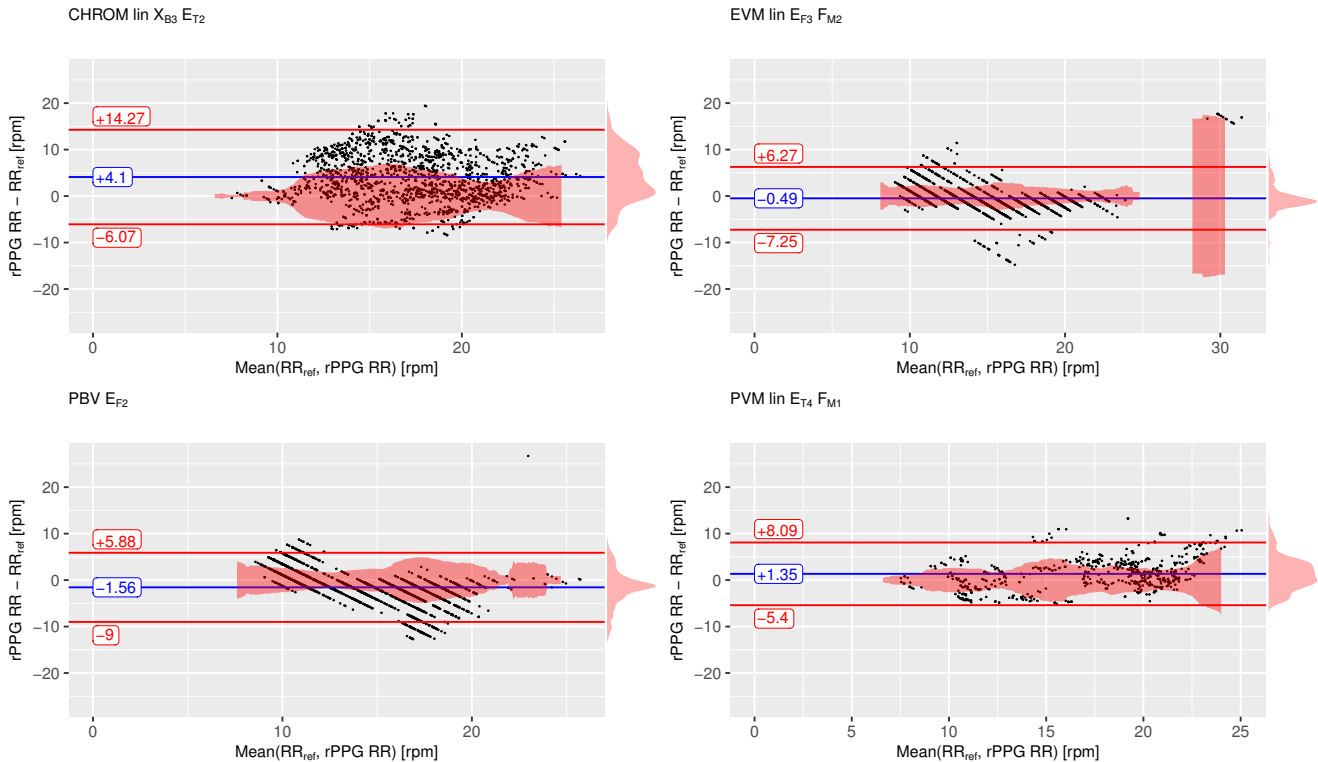


Figure 4. The Respiration scenario Bland Altman plot on four algorithms.

used is written after the combination algorithm. The F_* method is the optional modulation fusion method used by the pipeline. These algorithms are chosen to have one pipeline per combination algorithm. The complete pipeline was chosen considering all the metrics. The CHROM and EVM pipeline has a better quality with Movement and Respiration database respectively. The PVM and PBV pipelines were chosen using the Respiration and HandGrip results respectively.

The graphs show that the EVM, PVM and PBV methods give cleaner results on the Respiration scenario. EVM has

some outliers and PBV have higher error levels at higher frequencies. The CHROM method has low plot quality. This is due to the use of the cardiac signal enhancement to get the respiratory signal. The Respiration database has more energy in the respiratory frequencies band than in the cardiac frequencies band. This permits the respiratory rPPG combination algorithms to get better results.

5. Conclusion and future work

In this paper we used Charlton's framework with rPPG based signals to improve the respiration rate estimation

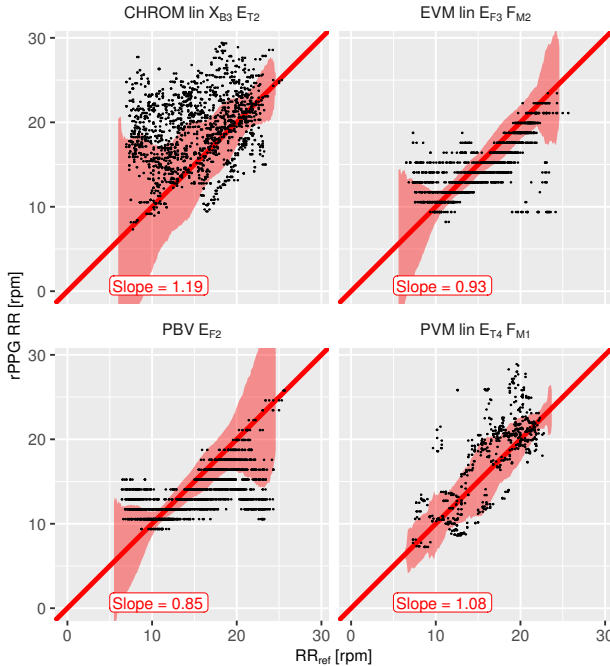


Figure 5. The Respiration scenario correlation plot on four algorithms.

quality. Some modifications were done to make it usable on rPPG signals. The framework was then tested on signals generated with four combination algorithms. These algorithms output either a cardiac rPPG signal or a respiratory rPPG signal. Then these signals were used as input to Charlton's framework. The respiratory signals (generated by the framework or by the combination) are then processed to detect a respiratory rate. This has shown that contact PPG algorithms can be used on rPPG signals to obtain accurate results. The estimation of the respiratory rate can be done with autoregressive models or time-domain analysis. The use of a modulation fusion step improves the results. Without the fusion step, the best algorithms used to get a respiratory signal are cardiac rPPG with *frequency modulation* or respiratory rPPG with *baseline wander*. A potential improvement of the method would be to choose the optimal algorithm depending on the color traces properties. Indeed, we showed that the best algorithm was either EVM on databases with high levels of respiratory signal or CHROM on cardiac signal combination with movement polluted signals. We also noticed that Respiration database signals have high respiration signal energy and low cardiac signal energy. This property can be assessed using a simple FFT on the color traces. In the Movement database, we can consider the movement noise level at the ROI tracking step. So another study should be done to show if it is possible to in-

crease the respiratory rate assessment quality by selecting the algorithm that fit the signals properties best.

References

- [1] Malcolm Elliott. Why is respiratory rate the neglected vital sign? A narrative review. *Int. Arch. Nurs. Health Care*, 2(3), June 2016.
- [2] Ian Smith, John Mackay, Nahla Fahrid, and Don Krueck. Respiratory rate measurement: A comparison of methods. *British Journal of Healthcare Assistants*, 5(1):18–23, Jan. 2011.
- [3] Lakshmiappathi Chelluri. Respiratory Deterioration and Cardiac Arrest. *Crit. Care Med.*, 47(1):71–72, Jan. 2019.
- [4] Bhupendra Shah, Bijay Bartaula, Janak Adhikari, Hari Shankar Neupane, Birendra Prasad Shah, and Guanraj Poudel. Predictors of In-hospital Mortality of Acute Ischemic Stroke in Adult Population. *J. Neurosci. Rural Pract.*, 8(4):591–594, Oct. 2017.
- [5] Craig Prescott and Stuart Ruff. The shocked patient. *Medicine*, 45(2):81–85, Feb. 2017.
- [6] Chien-Lung Shen, Tzu-Hao Huang, Po-Chun Hsu, Ya-Chi Ko, Fen-Ling Chen, Wei-Chun Wang, Tsair Kao, and Chia-Tai Chan. Respiratory Rate Estimation by Using ECG, Impedance, and Motion Sensing in Smart Clothing. *J. Med. Biol. Eng.*, 37(6):826–842, Dec. 2017.
- [7] Christian Steinberg, François Philippon, Marina Sanchez, Pascal Fortier-Poisson, Gilles O'Hara, Franck Molin, Jean-François Sarrazin, Isabelle Nault, Louis Blier, Karine Roy, Benoit Plourde, and Jean Champagne. A Novel Wearable Device for Continuous Ambulatory ECG Recording: Proof of Concept and Assessment of Signal Quality. *Biosensors*, 9(1):17, Mar. 2019.
- [8] Alessandra Fusco, Davide Locatelli, Francesco Onorati, Gianni Carlo Durelli, and Marco D. Santambrogio. On how to extract breathing rate from PPG signal using wearable devices. In *Biomedical Circuits and Systems Conference (BioCAS)*, pages 1–4. IEEE, Oct. 2015.
- [9] Harishchandra Dubey, Nicholas Constant, and Kunal Mankodiya. RESPIRE: A Spectral Kurtosis-based Method to Extract Respiration Rate from Wearable PPG Signals. In *IEEE/ACM International Conference on Connected Health: Applications, Systems and Engineering Technologies*, CHASE '17, pages 84–89, Philadelphia, Pennsylvania, Aug. 2017. IEEE.
- [10] Roxana Alexandra Cernat, Constantin Ungureanu, Georgeta Mihaela Ungureanu, Ronald Aarts, and Johan Arends. Real-time extraction of the respiratory rate from photoplethysmographic signals using wearable devices. page 17.
- [11] Fan Yang. Noncontact Detection of Respiration Rate Based on Forward Scatter Radar. *Sensors*, 19(21), 2019.
- [12] Guanghao Sun, Masakazu Okada, Rin Nakamura, Taro Matsuo, Tetsuo Kirimoto, Yukiya Hakozaki, and Takemi Matsui. Twenty-four-hour continuous and remote monitoring of respiratory rate using a medical radar system for the early detection of pneumonia in symptomatic elderly bedridden hospitalized patients. *Clinical Case Reports*, 7(1):83–86, 2019.

- [13] Michael H. Li, Azadeh Yadollahi, and Babak Taati. A non-contact vision-based system for respiratory rate estimation. In *2014 36th Annual International Conference of the IEEE Engineering in Medicine and Biology Society*, pages 2119–2122, Aug. 2014.
- [14] Kuan-Yi Lin, Duan-Yu Chen, and Wen-Jiin Tsai. Image-Based Motion-Tolerant Remote Respiratory Rate Evaluation. *IEEE Sensors Journal*, 16(9):3263–3271, May 2016.
- [15] Abbas K. Abbas, Konrad Heimann, Katrin Jergus, Thorsten Orlikowsky, and Steffen Leonhardt. Neonatal non-contact respiratory monitoring based on real-time infrared thermography. *BioMedical Engineering OnLine*, 10(1):93, Oct. 2011.
- [16] Sergey Yu Chekmenev, Helen Rara, and Aly A Farag. Non-contact, Wavelet-based Measurement of Vital Signs using Thermal Imaging. *ICGST*, page 6, Jan. 2006.
- [17] Serge Bobbia, Yannick Benerezeth, Duncan Luguern, Keisuke Nakamura, Randy Gomez, and Julien Dubois. Real-Time Temporal Superpixels for Unsupervised Remote Photoplethysmography. In *CVPM*, June 2018.
- [18] Magdalena Lewandowska, Jacek Ruminski, Tomasz Kocejko, and Jędrzej Nowak. Measuring Pulse Rate with a Webcam - a Non-contact Method for Evaluating Cardiac Activity. In *Federated Conference on Computer Science and Information Systems (FedCSIS)*, pages 405–410, Jan. 2011.
- [19] Mingliang Chen, Qiang Zhu, Harrison Zhang, Min Wu, and Quanzeng Wang. Respiratory Rate Estimation from Face Videos. In *2019 IEEE EMBS International Conference on Biomedical & Health Informatics (BHI)*, pages 1–4, May 2019.
- [20] Peter H Charlton, Timothy Bonnici, Lionel Tarassenko, Jordi Alastruey, David A Clifton, Richard Beale, and Peter J Watkinson. Extraction of respiratory signals from the electrocardiogram and photoplethysmogram: Technical and physiological determinants. *Physiol. Meas.*, 38(5):669–690, May 2017.
- [21] Ming-Zher Poh, Daniel J McDuff, and Rosalind W Picard. Advancements in Noncontact, Multiparameter Physiological Measurements Using a Webcam. *IEEE Trans. Biomed. Eng.*, 58(1):7–11, Jan. 2011.
- [22] Richard Macwan, Serge Bobbia, Yannick Benerezeth, Julien Dubois, and Alamin Mansouri. Periodic Variance Maximization Using Generalized Eigenvalue Decomposition Applied to Remote Photoplethysmography Estimation. In *Conference on Computer Vision and Pattern Recognition Workshops (CVPRW)*, pages 1413–1418, Salt Lake City, UT, June 2018. IEEE.
- [23] Duncan Luguern, Yannick Benerezeth, Virginie Moser, L. Andrea Dunbar, Fabian Braun, Alia Lemkadem, Keisuke Nakamura, Randy Gomez, and Julien Dubois. Remote photoplethysmography combining color channels with SNR maximization for respiratory rate assessment. In *ISMIC*, Japan, May 2020.
- [24] Reza Sameni, Christian Jutten, and Mohammad Bagher Shamsollahi. A deflation procedure for subspace decomposition. *IEEE Trans. Signal Process.*, 58(4):2363–2374, May 2010.
- [25] Gerard de Haan and Vincent Jeanne. Robust Pulse Rate From Chrominance-Based rPPG. *IEEE Trans. Biomed. Eng.*, 60(10):2878–2886, Oct. 2013.
- [26] Gerard de Haan and Arno van Leest. Improved motion robustness of remote-PPG by using the blood volume pulse signature. *Physiol. Meas.*, 35(9):1913–1926, Sept. 2014.
- [27] Peter H. Charlton, Timothy Bonnici, Lionel Tarassenko, David A. Clifton, Richard Beale, and Peter J. Watkinson. An assessment of algorithms to estimate respiratory rate from the electrocardiogram and photoplethysmogram. *Physiol. Meas.*, 37(4):610, 2016.
- [28] Mark van Gastel, Sander Stuijk, and Gerard de Haan. Robust respiration detection from remote photoplethysmography. *Biomed. Opt. Express*, 7(12):4941–4957, Dec. 2016.
- [29] L. G. Lindberg, H. Ugnell, and P. Å. Öberg. Monitoring of respiratory and heart rates using a fibre-optic sensor. *Med. Biol. Eng. Comput.*, 30(5):533–537, Sept. 1992.
- [30] Paul S. Addison and James N. Watson. Secondary transform decoupling of shifted nonstationary signal modulation components: Application to photoplethysmography. *Int. J. Wavelets Multiresolut Inf. Process.*, 02(01):43–57, Mar. 2004.
- [31] Ainara Garde, Walter Karlen, J. Mark Ansermino, and Guy A. Dumont. Estimating Respiratory and Heart Rates from the Correntropy Spectral Density of the Photoplethysmogram. *PLOS ONE*, 9(1):e86427, Jan. 2014.
- [32] W. Karlen, S. Raman, J. M. Ansermino, and G. A. Dumont. Multiparameter Respiratory Rate Estimation From the Photoplethysmogram. *IEEE Transactions on Biomedical Engineering*, 60(7):1946–1953, July 2013.
- [33] Christina Orphanidou, Susannah Fleming, Syed Ahmar Shah, and Lionel Tarassenko. Data fusion for estimating respiratory rate from a single-lead ECG. *Biomedical Signal Processing and Control*, 8(1):98–105, Jan. 2013.
- [34] Rangsal Ruangsuvana, Gordana Velikic, and Mark F. Bocko. Methods to extract respiration information from ECG signals. In *IEEE International Conference on Acoustics, Speech and Signal Processing*, pages 570–573, Mar. 2010.
- [35] Devy Widjaja, Carolina Varon, Alexander Dorado, Johan A. K. Suykens, and Sabine Van Huffel. Application of Kernel Principal Component Analysis for Single-Lead-ECG-Derived Respiration. *IEEE Transactions on Biomedical Engineering*, 59(4):1169–1176, Apr. 2012.
- [36] Jesús Lázaro Plaza. Non-invasive techniques for respiratory information extraction based on pulse photoplethysmogram and electrocardiogram. In *TUZ*, 2015.
- [37] Axel Schäfer and Karl W. Kratky. Estimation of Breathing Rate from Respiratory Sinus Arrhythmia: Comparison of Various Methods. *Ann Biomed Eng*, 36(3):476, Jan. 2008.
- [38] Julian F. Thayer, John J. Sollers, Elisabeth Ruiz-Padial, and Jaime Vila. Estimating respiratory frequency from autoregressive spectral analysis of heart period. *IEEE Engineering in Medicine and Biology Magazine*, 21(4):41–45, July 2002.
- [39] Syed Ahmar Shah, Susannah Fleming, Matthew Thompson, and Lionel Tarassenko. Respiratory rate estimation during triage of children in hospitals. *Journal of Medical Engineering & Technology*, 39(8):514–524, Nov. 2015.

- [40] Susannah Fleming, Lionel Tarassenko, Matthew Thompson, and David Mant. Non-invasive measurement of respiratory rate in children using the photoplethysmogram. In *2008 30th Annual International Conference of the IEEE Engineering in Medicine and Biology Society*, pages 1886–1889, Aug. 2008.
- [41] Susannah G. Fleming Lionel Tarassenko. A Comparison of Signal Processing Techniques for the Extraction of Breathing Rate from the Photoplethysmogram. *World Academy of Science, Engineering and Technology, Open Science Index* 6, 1(6):366–370, June 2007.
- [42] Syed Ahmar Shah and Lionel Tarassenko. *Vital Sign Monitoring and Data Fusion for Paediatric Triage*. Thesis, Oxford University, UK, 2012.
- [43] Susannah Fleming. *Measurement and Fusion of Non-Invasive Vital Signs for Routine Triage of Acute Paediatric Illness*. Thesis, Oxford University, UK, 2010.
- [44] Anders Johansson. Neural network for photoplethysmographic respiratory rate monitoring. *Med. Biol. Eng. Comput.*, 41(3):242–248, May 2003.
- [45] Christina Orphanidou, Oliver Brain, Jacques Feldmar, Shahab Khan, James Price, and Lionel Tarassenko. Spectral fusion for estimating respiratory rate from the ECG. In *2009 9th International Conference on Information Technology and Applications in Biomedicine*, pages 1–4, Nov. 2009.
- [46] MATLAB. *Version 9.5.0 (R2018b)*. The MathWorks Inc., Natick, Massachusetts, 2018.
- [47] Paul Viola and Michael Jones. Rapid Object Detection using a Boosted Cascade of Simple Features. In *Computer Society Conference on Computer Vision and Pattern Recognition CVPR*, volume 1, Kauai, HI, USA, 2001. IEEE.
- [48] Bruce Lucas and Takeo Kanade. An Iterative Image Registration Technique with an Application to Stereo Vision. In *International Joint Conference on Artificial Intelligence (IJCAI'81)*, volume 7, pages 121–130, Apr. 1981.
- [49] Michael J. Jones and James M. Rehg. Statistical Color Models with Application to Skin Detection. *Int. J. Comput. Vis.*, 46(1):81–96, Jan. 2002.
- [50] Leila Mirmohamsadeghi, Sibylle Fallet, Virginie Moser, Fabian Braun, and Jean-Marc Vesin. Real-Time Respiratory Rate Estimation using Imaging Photoplethysmography Inter-Beat Intervals. In *Computers in Cardiology (CinC)*, Sept. 2016.